The EBG-Based Biosensor for Setting the Appropriate Dialysis Time in Hemodialysis Process

Sina Rahmani Charvadeh, *Member, IEEE*, Mohammad Hosseinzadeh, and Javad Ghalibafan

***Abstract*—Microwave biosensors can be considered a non-invasive method for monitoring the water content and the waste material in the blood due to their continuous examination and real-time results. In this work, we present a novel method for setting an appropriate dialysis time, so that patients can receive better quality dialysis. The design proposes a biosensor integrated with dialysis tubes and is implemented using electromagnetic band gap structure in the ISM band. The tubes are passed from inside the pierced substrates and over the patches before and after dialysis. The sensor is used as a quality control to non-invasively monitor the amount of blood purification of hemodialysis patients using changes observed in relative permittivity of blood (58–64) by recording the transmission resonance frequency. Hence, it can be concluded that changes in blood's dielectric properties can be detected using a biosensor. Before fabrication, the proposed sensor is simulated and confirmed via the measurement setup. The sensitivity performance is obtained to be about 0.09 and 0.06 for two resonances of f1= 1.5 GHz and f2 = 3.78 GHz, allowing for the monitoring of the waste reduction rate during dialysis. Eventually, we propose a low cost, and non-destructive microwave biosensor without sampling process, while also providing the diagnosis principles for blood clearance rate due to the dual-band performance.**

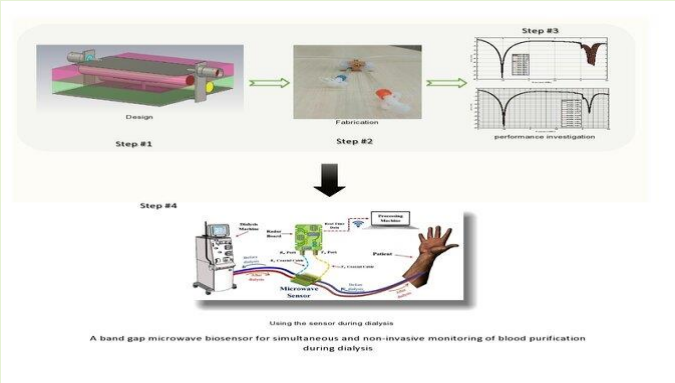

***Index Terms*—Electromagnetic band gap (EBG), Dual-band biosensor, Dialysis monitoring, Microwave method, Hemodialysis, Simultaneous dielectric detection**

I. Introduction

Kidney disease is a calamitous and grievous issue, and its expenditures to the international community are highly significant. In 2010, 2.62 million people worldwide suffered from kidney disease and the need for dialysis was anticipated to double by 2030 according to the Global Burden of Disease (GBD) [1]. In the U.S., about 26 million adult Americans have chronic renal disease [2]. The chronic kidney disease is described as prolonged kidney abnormalities, thus resulting in complications from another serious medical situation [3]. Accordingly, kidney failure is an end-stage of kidney disease, so that dialysis or a kidney transplant is the only treatment chance. Renal failure induces a gradual and progressive decrease in kidney function, and hence is susceptible to essential complications such as kidney failure and the total loss of kidney function [2]. Also, avoiding metabolic waste products will become feasible if the dialysis is continuously monitored and suitably done [4]. Based on the study performed by Jingjing Shi in 2020, regular dialysis monitoring via real-time of water content of blood measurement has been demonstrated to be a crucial appropriate dialysis time method to reduce the suffering of hemodialysis patients, in addition to the monitored organic and inorganic toxins [5].

In order to check the adequacy of dialysis levels, the definitive test for dialysis effectiveness used reliably by hemodialysis patients is to send blood samples to external laboratories for analysis after each session, which can take days for quantitative feedback. On the other hand, the cost, waste of time, and injury caused by the sampling process lead to considerable impetus for developing a non-invasive method, thus replacing blood sampling with monitoring of dialysis [6]. Hence, a novel requirement for non-invasive real-time dialysis quality monitors is preeminent to promote unceasing checks, thereby facilitating hemodialysis patients' care efficiently.

Substantial research has studied dialysis monitoring techniques continually, involving the dialysate using ultraviolet (UV) absorbance (where by decreases in the concentrations of solutes are determined using clearance UV technology) [7], and ionic dialysis [8], [9]. The ionic dialysis techniques use the low-frequency conductivity technique on dialysis to measure sodium levels in order to detect urea kinetics in blood [10], [11]. Nevertheless, high dialysate sodium changes arising from sodium loading is a general concern for ionic dialysis measurements [8]. Since the dielectric permittivity and conductivity of human blood change significantly during dialysis, the use of microwave monitoring techniques can be promising [4], [5], [12], [13].

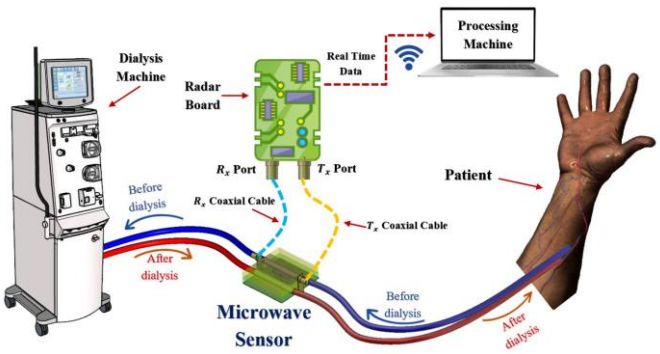

Fig. 1. Setting the appropriate dialysis time system using the proposed EBG sensing.`

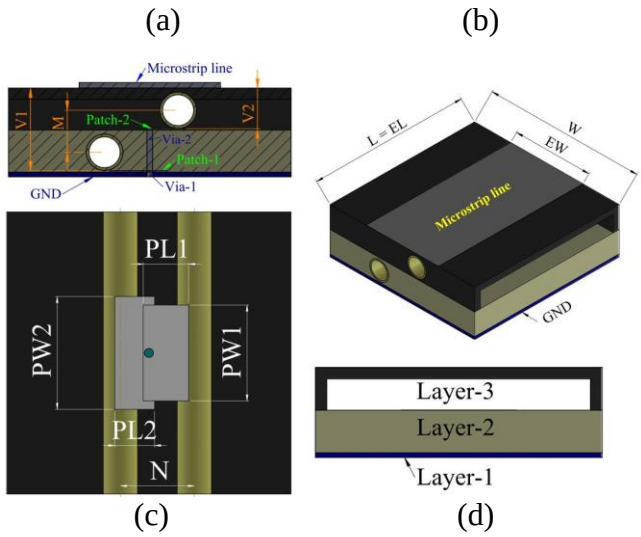

Fig. 2. Simulation of EBG structure: (a) front-view, (b) overview, (c) bottom-view, and (d) side-view.

In Ref. [13], using an open-ended coaxial probe method, the complex relative permittivity of blood was investigated in the frequency range of 0.2–6 GHz. In this case, an invasive method was employed, observing about 6 relative permittivity differences for patients before and after dialysis. However, the reported microwave techniques have not shown non-invasive methods for dialysis quality monitoring.

Here, we propose a band gap structure-based microwave sensing technique to develop a two-channel dual-band sensor for monitoring purposes during dialysis for the succeeding causes:

- Monitoring the dielectric properties of blood before and after dialysis using a low-power, low-cost structure.
- The sensor dimensions are in such a way that do not interfere with the dialysis process.
- The complete separation of the dialysis machine function that provides real-time measurements. Hence, it can be used for continuous monitoring.
- The EBG structures are proper for biosensors because they receive electromagnetic waves at high sensitivity [14].
- Two separate tubings are in different layers of the biosensor, thus achieving dual real-time sensing capability.

Fig. 1 shows the proposed sensing system for monitoring the blood during dialysis. In this way, we offer a dual-band microwave biosensor working in the ISM band, while also evaluating blood tubing before and after dialysis [15], [16]. Meanwhile, the sensitivity of the two tubings is independent from each other [17]- [19]. The sensing system consists of two different sizes of band gap patches placed in two separate substrates. The 50 Ω microstrip line feeds the supply at the ISM band.

The proposed biosensor can monitor the removal of metabolic waste from the blood (i.e., the water content of blood during dialysis and hematocrit), and timely setting appropriate dialysis. When the biosensor is implemented, the patient's blood before and after dialysis is loaded at a precise volume from inside the dialysis tube with the separate two-channel sensor. Removing waste materials and water in blood will decrease relative permittivity in the blood tube after dialysis. As a result, it will change the capacitance due to the coupling between the microstrip line and layer-1 patch. In turn, this enables the EBG biosensor to detect the water content of the blood (thus determining the appropriate time for dialysis) by detecting the depth/amplitude and/or changes in reflection frequency and transition resonances at the ISM frequency band. Various sensor simulations were performed in the time domain using CST Studio Suite 2021 (as full wave software). The equivalent circuit mode of the EBG structure was developed in Advanced Design System (ADS, 2021) software. The setup practically demonstrated the sensor performance for detecting the decreased blood permittivity of interest.

This paper is divided into five main sections: The proposed biosensor design, necessary simulations, and implementation of the prototype are explained in Section II. Section III involves the numerical simulations of the sensor for dialysis monitoring. Section IV presents the lab measurement results and the proposed setup. The last section finishes with conclusions and suggestions for future work.

II. Theory Of Hemodialysis Monitoring And Proposed Biosensor Responses

The biosensor configuration comprises three different substrates with the following specifications: thickness = h, width = W, and length = L. The 1- and 2-patches are located at distances of V1 and V2 from the microstrip line, respectively. A metal via is made for each EBG patch to create a current flow. Dialysis tubes are designed inside the substrates, and the center distance of tube-1 and 2 shown with M in Fig. 2. This structure is coupled with the length and width of the microstrip line, being equal to EL and EW located on the top face of the 3-substrate.

The electric field interacts with the blood tubes placed nearby EBG patches. Thus, each permittivity changes in the blood depends on the capacitance induced between the transmission line and layers. In this way, the monitoring dialysis principle for this EBG biosensor is based on the capacitance changes of substrates, arising from the reduction in the waste materials in the presence of the blood under

This article has been accepted for publication in IEEE Sensors Journal. This is the author's version which has not been fully edited and content may change prior to final publication. Citation information: DOI 10.1109/JSEN.2023.3289999

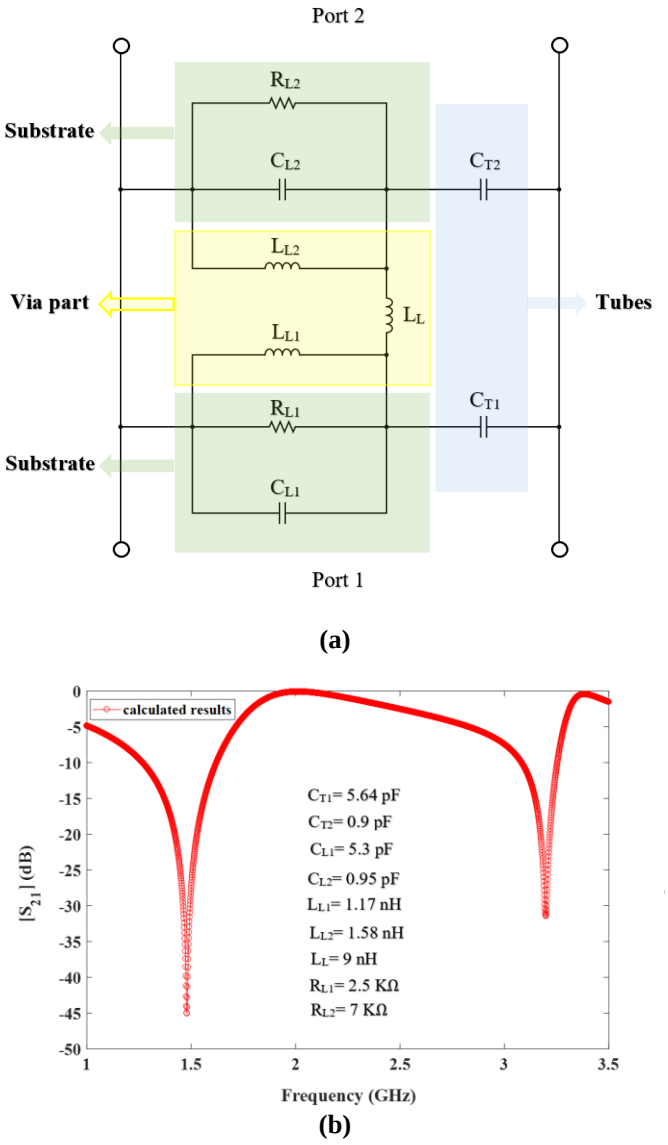

Fig. 3. Electrical Modelling of EBG structure: (a) the equivalent electrical model, and (b) the calculated results from the equivalent circuit in (a) by ADS software.

dialysis. This is exerted on the patch, so that the electric field interacts mostly with the tube at the resonance frequency. The outcome shift in transmission response is related to the blood permittivity, and associated with the waste material rate by the analysis of both the resonance frequency and corresponding peak attenuation.

A. Equivalent Circuit Model

To describe the physical behavior of EBGs, it is possible to use the circuit model based on lumped elements. With the purpose of electrically modeling the EBGs, the microstrip line was developed based on RLC elements in the equivalent electrical circuit, as shown in Fig. 3 [20]. Inductances L_{L1}, L_{L2}, and L_{L3} were used to model the current flow of metal via when connecting the patch for excitation. The capacitance C_{L1} can model the dielectric layer-1 EBG patch, guiding the EM fields to be coupled with the ground plane. The capacitance C_{L2} is responsible for the layer-2 EBG patch and ground plane. The losses of the lower substrate are represented by R_{L1}. R_{L2} is the equivalent resistance of layer-2 and layer-1 and the contact between them. C_{T1} is equivalent to tube-1, whose changes affect the capacitance between the transmission line and layer-1. Similarly, C_{T2} is the same as tube-2, whose capacitance corresponds to the transmission line and layer-2. By changing the dielectric materials of tubes-1 and 2, the capacity of C_{T1} and C_{T2} can be changed. Consequently, changes in the dielectric characteristics of the blood are reflected into f1 and f2. Given this structure, the first (fc1) and second (fc2) resonances are given by [21]:

$$f1 = \frac{1}{2\pi\sqrt{L_{L1}\left(C_{T1}+C_{L1}\right)}} \quad (1)$$

$$f2 = \frac{1}{2\pi\sqrt{L_{L2}\left(C_{T2}+C_{L2}\right)}} \quad (2)$$

In continuance, the electrical modelling of the EBG structure is described in Fig. 3(a). Fig. 3(b) shows the results of the equivalent circuit calculated by ADS software. According to the results obtained, there are two independent resonant frequencies (1.48 GHz and 3.2 GHz) that provide independent simultaneous monitoring of tubes.

B. Proposed Biosensor Design and Fabrication

Before implementation, we used the CST Studio Suite 2021 to design the proposed EBG biosensor illustrated in Fig. 2. Three substrates were utilized of length L = 50 mm, width W = 50 mm, and thickness h = 13.8 mm. The layer-1 of a RO4003C dielectric substrate (ε_r = 3.55 and tanδ = 0.0027) with thickness h1 = 0.8 mm, and middle substrate composed of Teflon material with the following specifications: dielectric constant ε_r = 2.1, loss tangent tanδ = 0.0002, and thickness h2 = 6.5 mm were used in biosensor design. The last layer was selected to be a hollow optical plexiglass box in order to implement the transmission line (L = EL and EW = 25 mm). Also, the box bottom wall and the sidewalls that did not harm the tube mechanical strength were removed, so that ε_r of layer-3 became similar to that of air. Also, the box bottom wall and the sidewalls that did not harm the tube mechanical strength were removed, so that ε_r of layer-3 became similar to that of air. Two identical vias with radii of r = 1 mm were created and located precisely in the center of the W×L. Patch-1 and 2 with dimensions of PW1 = 20 mm × PL1 = 7 mm and PW2 = 17 mm × PL2= 8 mm, and with height from transmission line of V1 = 12.44 mm and V2 = 6.44 mm, were optimized to create independent sensitivity. The diameter of the tube, similar to the real dialysis tube, was considered to be 6 mm. The tubes that are supposed to be monitored before and after dialysis are embedded in the sensor with a height of M = 6.25 mm and a distance of N = 13 mm with respect to each other. The general configuration of the sensor can be seen in Fig. 2.

A laboratory sample of the biosensor was fabricated using 0.06 mm copper layers for all purposes. On the other hand, a CNC device was initially used to etch holes inside layer-2 and

3 to pass hemodialysis tubes properly. Subsequently, the optical plexiglass box was designed on Teflon material using 3D scanning, and a laser was used to cut the sidewalls after regulation with the layer-2. The multiple views of the fabricated biosensor are shown in Fig. 4.

C. Principles of Performance

The complex permittivity of blood changes considerably for a variable level of waste materials from hemodialysis patients (having relative permittivity of 58-64). For instance, the invasive measurement method in Refs. [5] and [13] indicates that the percent change in ε_r is around 10% at the ISM band by performing hemodialysis. Therefore, for hemodialysis monitoring applications, we design a biosensor to investigate blood sent and returned to the machine, while also comparing these two types of blood. In this way, the amount of reduction in the waste materials during dialysis is determined, the data obtained from blood monitoring before and after dialysis can be compared, and a decision is made about the quality of dialysis performed. In this case, when the blood enters the biosensor, it has a relatively high permittivity due to the waste materials. At each dialysis stage, the relative permittivity decreases, and blood returns to the sensor. There will be a difference between the input blood of the first and second states, which determines the rate of relative permittivity reduction in each dialysis step. By obtaining this reduction rate through monitoring the blood before and after dialysis, it is possible to determine the appropriate time for dialysis. For this reason, two independent resonances were used.

Alternatively, the use of two independent resonances for the simultaneous detection of dielectric properties of materials can have some advantages such as improvement in the size of biosensors, reduction in the number of measurement times (thus reducing measurement errors), and increase in the accuracy of dielectric properties measurement. However, a material can be better described by using two independent frequencies because its complex permittivity is a function of frequency and the greatest changes occur in the microwave region. The simultaneous detection of changes with two independent resonances makes it possible to use only the transmission coefficient parameter to detect changes in the dielectric properties of blood, and no other criteria will be needed. As a result, the biosensor will have a single sensing region for two independent resonances. Nonetheless, dual-band sensors usually use multiple dielectric substrates to create independent resonance, which poses challenges in the fabrication process. The simulation of the sensor and how it works will be investigated in the next section.

III. Hemodialysis Monitoring Simulation

Prior to the measurement, the performance of the EBG biosensor was simulated for non-invasive monitoring of dialysis. Solution samples were used in this investigation to mimic different relative permittivity of blood relevant to the hemodialysis process. Blood samples of relative permittivity in the range of 58–64 were simulated inside the tube sensing region. This study investigated blood dielectric properties in relation to the resonances of the EBG biosensor in the CST software. Expressly, we utilized approximate dielectric permittivity parameters for the blood samples of interest at the ISM band as listed in Table I. Synthetic blood was obtained to investigate the permittivity dependence using a Vector Network Analyzer (VNA) and Keysight material analyzer (N1501A). Therefore, the permittivity of the synthetic blood samples was extracted by Eq (3), employing the relative permittivity of water ($\varepsilon_{r\omega}$), the relative permittivity of other materials excluding water in the synthetic blood (ε_{rm}), and α (i.e., the water content of synthetic blood) [5].

$$\varepsilon_r = \varepsilon_{r\omega}{}^{\alpha}\, \varepsilon_{rm}{}^{1-\alpha} \tag{3}$$

First, the blood inside the two tubes with ε_r = 64 was considered, resulting in the transmission response presented in Fig. 5. The simulated transmission responses for the various selections of B1–B13 loaded at tubes (each volume equals to 6 μL) are shown in Fig. 6. The results show the variations of |S21| at different dialysis times, being proportional to the decrease in blood permittivity. To mimic the dialysis machine behavior when clearing the blood, we initially decreased the relative permittivity of the tube after dialysis, followed by

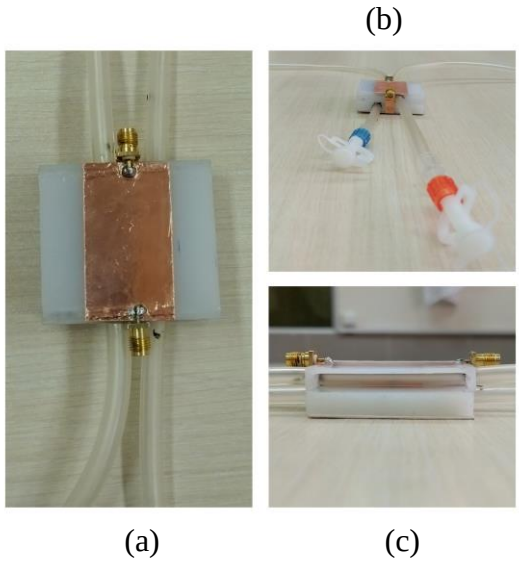

Fig. 4. The fabricated biosensor prototype: (a) top-view depicting the microstrip line, (b) front-view showing the dialysis tubes, and (c) side-view showing the layers.

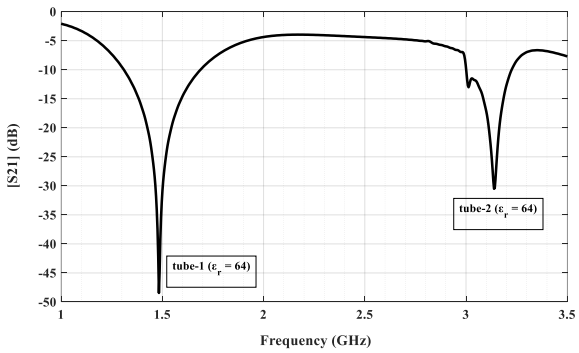

Fig. 5. Simulated transmission coefficient of EBG at the dialysis start mode.

reducing it before dialysis. Fig. 6 shows that at f = 1.48 GHz and f = 3.13 GHz, the biosensor response is recorded over the ISM band with two independent resonances. Each of the resonances is related to one of the tubes, so that the blood purification rate can be extracted by comparing between the obtained data. To observe two independent resonances, the permittivity of tube-1 changes with variables B1-B13 by keeping the contents of tube-2 constant, according to Fig. 6(a). This was repeated for tube-2, as shown in Fig. 6(b). The obtained deduction indicates that the appropriate dialysis time could be adjusted by using the proposed biosensor. In the next part of this research, we will examine the sensor measurement and detection performance to confirm the simulation results.

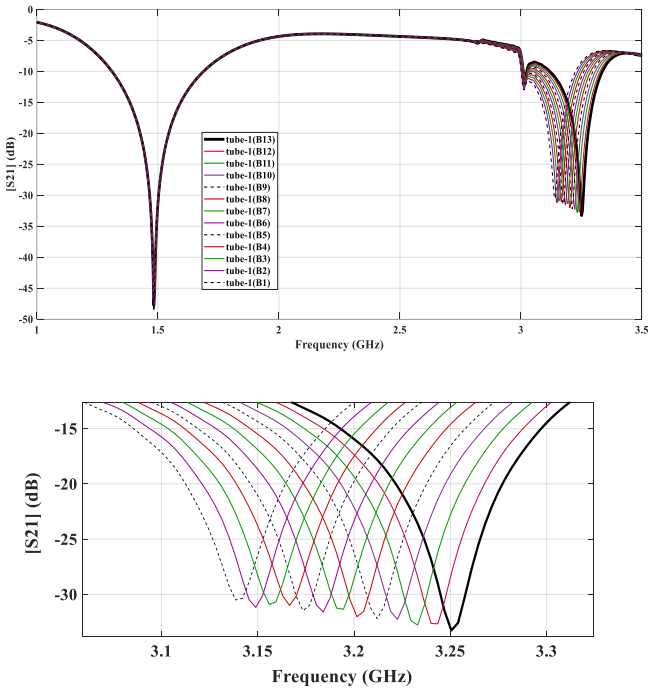

(a)

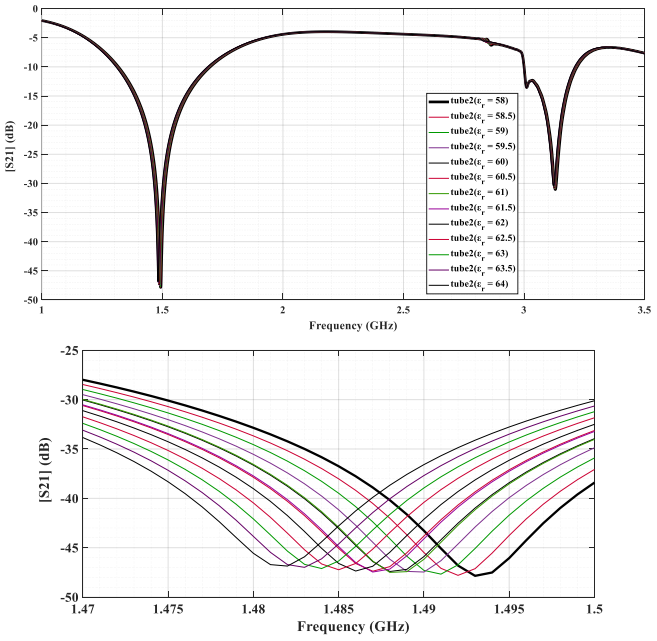

(b)

Fig. 6. The simulated transmission response of the EBG loaded with samples B1–B13: (a) by keeping the contents of tube-2 constant, the permittivity of tube-1 changes with variables B1-B13. (b) Similar to (a), by keeping the contents of tube-1 constant, the permittivity of tube-2 changes with variables B1-B13.

IV. Measurement Results for Dialysis Monitoring

The fabricated EBG prototype was experimented in order to monitor the purification rate in synthetic waste material-based blood. To simulate the dialysis machine behavior, the synthetic blood was prepared in disparate samples with relative permittivity of 58, 61.4, and 64.6 at a volume of 50 mL in the lab. For this purpose, distilled water was combined with industrial alcohol solution to achieve the relative permittivity of interest. As a result, fake blood was prepared using a combination of distilled water and industrial alcohol to confirm the performance of the biosensor.

Fig. 7 depicts the experimental setup, where the EBG biosensor is connected to VNA. Therefore, S21 of the biosensor can be measured by the frequency shift. VNA was calibrated by the Open-Short-Load technique before connecting the biosensor, and set at ambient temperature (25 ºC) and 1600 frequency points. At the start of dialysis, S21 of the EBG structure was measured and confirmed as schemed in Fig. 8. Next, the biosensor was experimented to detect the decreased relative permittivity in the three prepared samples of 64.6, 61.4, and 58. Each of the prepared samples was measured three times to confirm repeatability. The average of the three repeated measurements for the corresponding blood sample is the result of each scattering plot in Fig. 8. After each reduction of ε_r = 6, obvious changes were observed in transition resonances towards lower frequencies, indicating the resonance frequency dependence on the sample's permittivity. The synthetic blood permittivity changes were reflected as the resonance peak set towards the ISM band (transmission coefficients over the band 1–4 GHz in Fig. 8), thereby confirming the biosensor ability to detect decreasing variations in the relative permittivity of the tested samples.

Furthermore, the sensitivity of the proposed EBG biosensor for dialysis monitoring was investigated by assuming the frequency shift as a sensing parameter. Absolute change in the magnitude of S21 is considered to be the biosensor sensitivity at any of the resonances corresponding to the change in permittivity. For two resonances, the maximum sensitivity was calculated using Eq. (4), as given below [22], [23]:

$$\%S = \frac{f_s - f_0}{f_0\left(\varepsilon_r - 1\right)} \times 100 \tag{4}$$

where %S is the sensitivity, f_0 denotes the first resonance frequency for the biosensor, and f_s represents the resonance frequency for the blood sample inside the tube with ε_r. The maximum sensitivity at the measured resonances of f1= 1.5

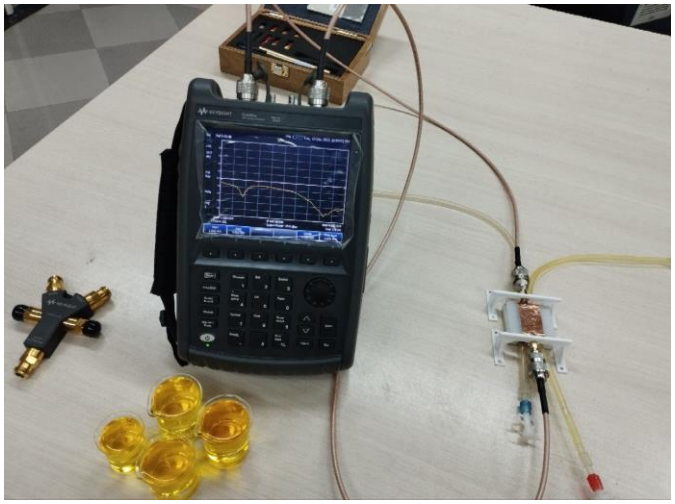

Fig. 7. Experimental setup to detect changes in dielectric properties rate of blood.

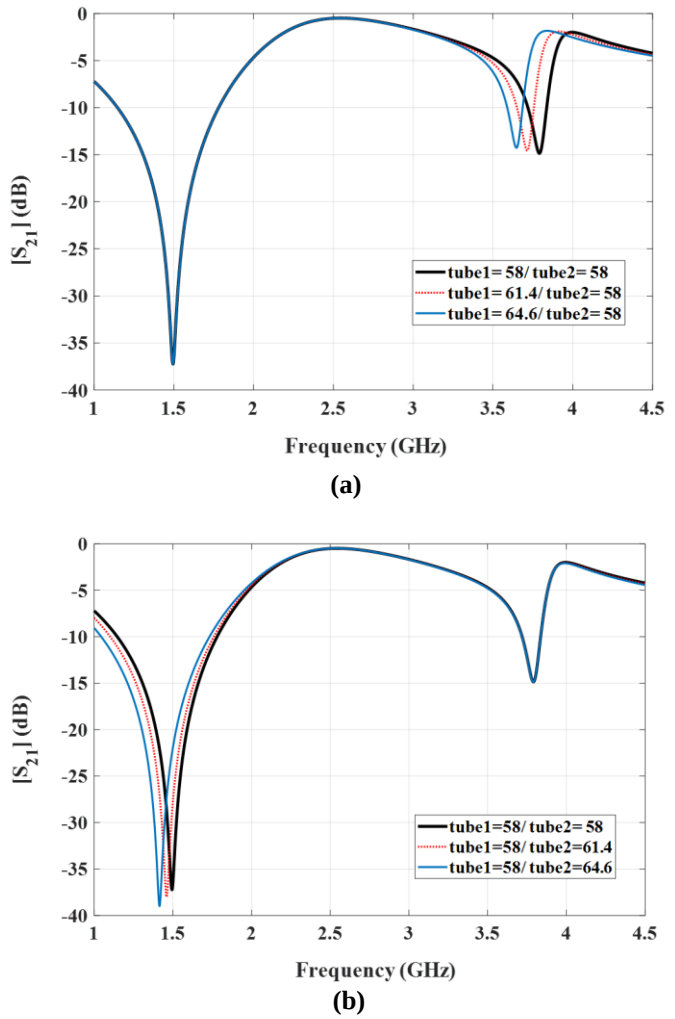

Fig. 8. $|S_{11}|$ measured at 1–4 GHz for tested blood samples: (a) keeping the contents of tube-2 constant leads to changes in the permittivity of tube-1. (b) The opposite of the previous situation.

GHz and f2 = 3.78 GHz is estimated to be 0.09 and 0.06, respectively. As can be inferred, the second resonance has a higher frequency shift than the first resonance.

Lastly, Table II produces a comparative review of microwave sensors with their respective parameters: operating frequency, sensing parameter, sensitivity, technology, and application. Careful investigation of Table II clearly demonstrates that the proposed EBG biosensor has advantages such as independent dual-band, frequency independence, and wide frequency range that outperforms other techniques and mechanisms in the literature for microwave sensing. Especially, The EBG-based biosensor can accurately detect small variations of the waste materials in the blood with relatively high sensitivity.

V. Conclusion

This study has presented the first microwave biosensor operating in the ISM band for monitoring dialysis. The sensing method was implemented using EBG structure in three layers of different materials. The placement of dialysis tubes in each sensor layer made it possible to create independent dual-band monitoring. The sensor capability for detection of the metabolic waste reduction rate was verified by the blood samples integrated with EBG biosensor, where the patches had a high-focus electric field. The relative permittivity changes of the loaded blood samples led to the difference in each substrate capacitance, resulting in detectable variations in the resonances proportional to the blood permittivity. To validate the performance of the implemented biosensor, permittivity variation of synthetic blood was measured to be in the range of 58–64. The sensor sensitivity to waste material changes had sensitivity percentages of about 0.09 and 0.06 in |S21|. The proposed biosensor provided the excellent potential for integration with dialysis machines to set appropriate dialysis times as non-invasive monitoring in real-time.

In future, novel microwave methods can be offered for investigating dialysis adequacy for hemodialysis patients, thereby benefiting them more effectively. For example, non-invasive measurement of urea variation rate during dialysis can be attractive and important using biosensors. However, the investigation of patients with different attributes of blood will remain ambiguous, thus requiring more information extraction.

References

[1] V. Luyckx, M. Tonellib and J. W. Stanifer, "The global burden of kidney disease and the sustainable development goals," *Bull. World.*, vol. 96, no. 6, pp. 414-422c, 2018, doi:10.2471/BLT.17.206441.

[2] N. u. Amin, R. T. Mahmood, M. J. Asad, M. Zafar and A. M. Raja, "Evaluating Urea and Creatinine Levels in Chronic Renal Failure Pre and Post Dialysis: A Prospective Study," *J. Cardiovasc. Dis.*, vol. 2, no. 2, , pp. 2330-4596, 2014.

[3] K. H. Kim, M. S. Lee, T.-H. Kim, J. W. Kang, T.-Y. Choi and J. D. Lee, "Acupuncture and related interventions for symptoms of chronic kidney disease," *Cochrane Database Syst Rev.*, vol. 28, no. 6, p. 128, 2016, doi: 10.1002/14651858.CD009440.pub2.

[4] P. D. Jensen, P. M. Meaney, N. R. Epstien and K. D. Paulsen, "Cole–Cole Parameter Characterization of Urea and Potassium for Improving Dialysis Treatment Assessment," in IEEE Antennas and Wireless Propagation Letters, vol. 11, pp. 1598-1601, 2012, doi: 10.1109/LAWP.2012.2237536.

[5] J. Shi, S. Seo and J. Wang, "Monitoring Water Content of Blood During Hemodialysis Based on Complex Permittivity Measurement," *IEEE Sens. J.*, vol. 20, no. 13, pp. 7347-7353, July 1, 2020, doi: 10.1109/JSEN.2020.2978220.

[6] I. T. Degim, S. Ilbasmis, R. Dundaroz and Y. Oguz, "Reverse iontophoresis: a non-invasive technique for measuring blood urea level," *Pediatr Nephrol*, vol. 18, no. 10, pp. 1032-1037, Jul, 2003, doi: 10.1007/s00467-003-1217-y.

[7] G. Vasquez-Rios, F. Zhang, M. G. Scott and A. Vijayan, "Adequacy of hemodialysis in acute kidney injury: Real-time monitoring of dialysate ultraviolet absorbance vs. blood-based Kt/Vurea," *Hemodial Int.*, vol. 25, no. 1, p. 4349, 2021, doi: 10.1111/hdi.12879

[8] S. Aslam, S. J. Saggi, M. Salifu and R. J. Kossmann, "Online measurement of hemodialysis adequacy using effective ionic dialysance of sodium-A review of its principles, applications, benefits, and risks," *Hemodial Int.*, vol. 22, no. 4, pp. 425-434, 2018, doi: 10.1111/hdi.12623.

[9] A. Rodriguez, M. Morena , A. S. Bargnoux, L. Chenine, H. Leray-Moragues, J. P. Cristol,B. Canaud, "Quantitative assessment of sodium mass removal using ionic dialysance and sodium gradient as a proxy tool: Comparison of high-flux hemodialysis versus online hemodiafiltration," *Artif Organs.*, vol. 45, no. 8, pp. E280-E292, 2021, doi: 10.1111/aor.13923.

[10] M. Berger, F. Sellering, H. Röhrich, H. Mansour, T. Perl and S. Zimmermann, "A Differential Transformer for Noninvasive Continuous Sodium Monitoring During Dialysis Treatment," *2019 IEEE SENSORS*, Montreal, QC, Canada, 2019, pp. 1-4, doi: 10.1109/SENSORS43011.2019.8956610.

[11] W. -M. Chi, B. -M. Ju and S. -Y. Huang, "Using Bioelectrical Impedance Vector Analysis Method Estimate the Hydration State during Hemodialysis," *2020 IEEE Eurasia Conference on IOT, Communication and Engineering (ECICE)*, Yunlin, Taiwan, 2020, pp. 28-31, doi: 10.1109/ECICE50847.2020.9301951.

[12] Z. Ramsaroop, S. Rocke, N. Gayapersad and J. Persad, "CSRR-based microwave sensor for noninvasive, continuous monitoring of renal function," *2016 Loughborough Antennas & Propagation Conference (LAPC)*, Loughborough, UK, 2016, pp. 1-5, doi: 10.1109/LAPC.2016.7807584.

[13] A. Takeda, K. Takata, H. Nagao, J. Wang and O. Fujiwara, "Measurement and Hemodialysis Effect of Complex Relative Permittivity for Blood of Kidney Patients Using Open-Ended Coaxial Measurement Probe," *Electronics and Communications in Japan (ECJ)*, vol. 95, no. 12, pp. 56-61, 2012, doi: 10.1002/ecj.11421.

[14] R. Yadav and P. N. Patel, "Experimental Study of Adulteration Detection in Fish Oil Using Novel PDMS Cavity Bonded EBG Inspired Patch Sensor," *IEEE Sens. J.*, vol. 16, no. 11, pp. 4354-4361, June1, 2016, doi: 10.1109/JSEN.2016.2542287.

[15] C. G. M. Ryan and G. V. Eleftheriades, "Single- and Dual-Band Transparent Circularly Polarized Patch Antennas With Metamaterial Loading," *IEEE Antennas Wirel. Propag. Lett.*, vol. 14, pp. 470-473, 2015, doi: 10.1109/LAWP.2014.2368115.

[16] S. Y. Jun, B. Sanz Izquierdo and E. A. Parker, "Liquid Sensor/Detector Using an EBG Structure," *IEEE Trans. Antennas Propag.*, vol. 67, no. 5, pp. 3366-3373, May 2019, doi: 10.1109/TAP.2019.2902663.

[17] H. Zhou, D. Hu, C. Yang, C. Chen, J. Ji, M. Chen, Y. Chen, Y. Yang, X. Mu, "Multi-Band Sensing for Dielectric Property of Chemicals Using Metamaterial Integrated Microfluidic Sensor," *Sci Rep.*, 2018, doi: 10.1038/s41598-018-32827-y.

[18] S. Roy and U. Chakraborty, "Metamaterial-embedded dual wideband microstrip antenna for 2.4 GHz WLAN and 8.2 GHz ITU band applications," *Waves Random Complex Media*, vol. 30, no. 2, 2018, doi: 10.1080/17455030.2018.1494396.

[19] S. C. Mukhopadhyay, "Smart Sensors, Measurement and Instrumentation," Sydney, NSW, Springer, 2021.

[20] D. H. Lee, J. H. Kim, J. H. Jang, W. S. Park, " Dual-frequency dual-polarization antenna of high isolation with embedded mushroom-like EBG cells, " *Opt. Lett.*, vol. 49, no. 7, pp. 1764-1768, Apr. 2007, doi:10.1002/mop.22513.

[21] P. P. Bhavarthe, S. S. Rathod and K. T. V. Reddy, "A Compact Dual Band Gap Electromagnetic Band Gap Structure," *IEEE Trans. Antennas Propag.*, vol. 67, no. 1, pp. 596-600, Jan. 2019, doi: 10.1109/TAP.2018.2874702.

[22] A. Ebrahimi, W. Withayachumnankul, S. Al-Sarawi and D. Abbott, "High-Sensitivity Metamaterial-Inspired Sensor for Microfluidic Dielectric Characterization," *IEEE Sens. J.*, vol. 14, no. 5, pp. 1345-1351, May 2014, doi: 10.1109/JSEN.2013.2295312.

[23] W. Ye, D. -W. Wang, J. Wang, S. Chen, G. Wang and W. -S. Zhao, "An Ultrahigh-Sensitivity Dual-Mode Microwave Sensor for Microfluidic Applications," *IEEE Microw. Wirel. Compon. Lett.*, doi: 10.1109/LMWT.2023.3252008.

[24] A. Ali, B. Hu, and O. Ramahi, “Intelligent Detection of Cracks in Metallic Surfaces Using a Waveguide Sensor Loaded with Metamaterial Elements,” *Sensors*, vol. 15, no. 5, pp. 11402–11416, May 2015, doi: 10.3390/s150511402.

[25] Q. Wang et al., "High-Sensitivity Dielectric Resonator-Based Waveguide Sensor for Crack Detection on Metallic Surfaces," *IEEE Sens. J.*, vol. 19, no. 14, pp. 5470-5474, 15 July15, 2019, doi: 10.1109/JSEN.2019.2907129.

[26] M. C. Cebedio, L. A. Rabioglio, I. E. Gelosi, R. A. Ribas, A. J. Uriz and J. C. Moreira, "Analysis and Design of a Microwave Coplanar Sensor for Non-Invasive Blood Glucose Measurements," *IEEE Sens. J.*, vol. 20, no. 18, pp. 10572-10581, 15 Sept.15, 2020, doi: 10.1109/JSEN.2020.2993182.

[27] P. Mohammadi, A. Mohammadi, S. Demir and A. Kara, "Compact Size, and Highly Sensitive, Microwave Sensor for Non-Invasive Measurement of Blood Glucose Level," *IEEE Sens. J.*, vol. 21, no. 14, pp. 16033-16042, 15 July 15, 2021, doi: 10.1109/JSEN.2021.3075576.

This article has been accepted for publication in IEEE Sensors Journal. This is the author's version which has not been fully edited and content may change prior to final publication. Citation information: DOI 10.1109/JSEN.2023.3289999

Sina Rahmani Charvadeh (Member, IEEE) was born in Iran, in 1998. He received the B.Sc. degree in electrical engineering from the University of Mohaghegh Ardabili, Ardabil, Iran, in 2020, and the M.Sc. degree in electromagnetic fields & waves in electrical engineering from the Faculty of Electrical Engineering, Shahrood University of Technology, Shahrood, Iran, in 2022. His main research interests include microwave techniques in modern medical applications; biosensors; microwave sensors; antenna and microwave devices; microwave ablation; Health care; permittivity measurement; dielectric materials; and metamaterial.

Mohammad Hosseinzadeh obtained his B.Sc. degree from the Shahrood University of Technology, Shahrood, Iran, in 2021. Currently, he is pursuing his M.Sc. degree in Electrical Engineering from the same institution. His research interests are millimeter wave devices, metamaterials, antenna design, and passive and active microwave devices.

Javad Ghalibafan received the B.S. degree from the Ferdowsi University of Mashhad in 2007 and the M.S. and Ph.D. degrees from Iran University of Science Technology in 2009 and 2013, respectively. In 2014, he joined Faculty of Electrical and Robotic Engineering, Shahrood University of Technology, Shahrood, Iran, where he is now Associate Professor, and the head of Antenna & Microwave Lab. His research interests include the analysis, design, and measurement of artificial electromagnetic materials; antenna and microwave devices; metamaterial; and magnetic material.

TABLE I
VARIATION IN DIELECTRIC PROPERTIES OF BLOOD DURING DIALYSIS FOR SAMPLES B1–B13.

Blood samples	**B1**	**B2**	**B3**	**B4**	**B5**	**B6**	**B7**	**B8**	**B9**	**B10**	**B11**	**B12**	**B13**
ε_r	64	63.5	63	62.5	62	61.5	61	60.5	60	59.5	59	58.5	58

TABLE II
COMPARISON OF THE PROPOSED BIOSENSOR WITH OTHER MICROWAVE SENSORS

Ref.	**Operation frequency (GHz)**	**Sensing parameter**	**Sensitivity**	**Technology**	**Application**
[24]	12–18	$\|S_{11}\|$, single band	Low	Waveguide Sensor	Crack detection in metallic surfaces
[25]	14-18	$\|S_{11}\|$, single band	Medium	Waveguide Sensor	Crack detection in metallic surfaces
[26]	1.5 – 2.5	$\|S_{11}\|$, single band	Medium	Microwave Coplanar Sensor	Measuring blood glucose levels
[27]	2.275 - 2.5515	$\|S_{21}\|$ and $\|S_{31}\|$, single band	High	Branch line coupler and split ring resonators	Measuring blood glucose levels
This work	1 - 4	$\|S_{21}\|$, dual independent band	High	EBG biosensor	monitoring dialysis